2010 IEEE-RAS International Conference on Humanoid Robots
Nashville, TN, USA, December 6-8, 2010

Stabilization of a hopping humanoid robot for a push

Baek-Kyu Cho[1], Sang-Sin Park[2] and Jun-ho Oh[3]

[1] *ATR, Japan, swan0421@gmail.com*

[2]*KAIST, Republic of Korea,momumima@kaist.ac.kr*

[3]*KAIST, Republic of Korea, jhoh@kaist.ac.kr*

Abstract— **This paper discusses the stabilization of a hopping humanoid robot for a push. According to the size of push, two controllers are selected. The posture balance controller is used when the push is small, and the posture balance controller and the foot placement method are activated together when the push is large. To develop the novel controller of the foot placement method, the simplified model is used and linearized Poincare map for single hopping is made. The control law is designed by the pole placement method. The proposed method is verified through the simulation and experiment. In the experiment, HUBO hops well against various pushes.**

I. Introduction

Many humanoid robots have been developed and various studies are going on. However, the basic and essential study for a humanoid robot is a research of locomotion. A humanoid robot has to maintain stability without regard to locomotion such as walking, hopping and running. Therefore, the stabilization of a humanoid robot is very important topic.

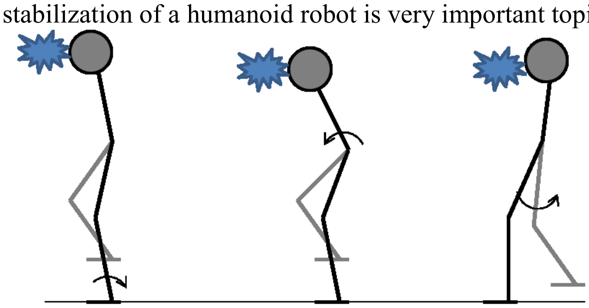

Figure 1. the three stabilization methods

The stabilization method of the humanoid robot for disturbance can be classified into three strategies, which are ankle torque strategy (a), reactive momentum strategy (b), and foot placement strategy (c) [1]. The ankle torque strategy is a basic method which the robot uses only torque of ankle joints to maintain stability. It is intuitive and easy to use because the robot maintains a balance via generating opposite ankle torque with respect to the falling direction. Also, reactive momentum strategy uses an angular momentum of COM of the robot. It prevents falling down with reactive momentum, for example, the swing of arms or torso.

On the other hand, in other point of view, a general method to stabilize a humanoid robot is to control a Zero moment point (ZMP) of the robot [2-4]. The ZMP is always controlled to be placed within the supporting polygon, that is, the sole of the stance foot. According to interpretation, it can be considered that the ZMP strategy is a combination of the ankle torque strategy and the reactive momentum strategy. Since a humanoid robot is redundant system consisting of many links, there are many kinds of cases to control a balance. For example, the ZMP can be controlled by only an ankle torque, only the motion of torso, or the combination of ankle torque and the motion of torso.

However, this ZMP strategy is not perfect. Even though a humanoid robot can maintain a balance with the ZMP control against small disturbance, it is very difficult to maintain stability with the ZMP control when large disturbance such as push is applied to the robot.

Therefore, a foot placement strategy is required. In the ZMP point of view, it means that the supporting polygon of the robot is changed instantly. In 2009, Toyota's Partner Robot demonstrated the push recovery experiment through the foot placement strategy. J. Pratt et al. calculated a capture region with a linear inverted pendulum model attached a flywheel, and verified it with a simulation of a simple model [5]. A. Kuo used a change of a foot placement for passive dynamic walking [6]. Also, Hyon et al. used a symmetric method which an angle of swing leg is the same as an angle of stance leg with respect to the vertical line from ground [7]. And, M. Raibert developed 3-dimensional biped being able to hop and run [8]. Even though, many studies for the foot placement have been carried out, the Partner robot is the only one to use the foot placement strategy among the human-sized humanoid robots. Hyon et al. applied the foot placement method to the human-sized robot. However, this method used when the robot didn't moved but stood up [9].

Therefore, in this paper, we propose the novel stabilization method against disturbance like push when a humanoid robot hops in place. And it is verified by an experiment. According to the size of push, the ankle torque strategy and the foot placement strategy are selected to stabilize. Theoretically the robot can make a balance with only the foot placement method. However, it is difficult to make a balance with only the foot placement method because the sensor signal drifts in the real environment and a sensor noise is generated from the impact when the robot lands on the ground.

The ankle torque strategy for small disturbance comes from the previous study [10]. On the other hand, the foot placement strategy for large disturbance is developed through following procedure. First, the humanoid robot is simplified as the model consisting 4 links, 3 masses, and 3 actuators. Second, the Poincare map is generated for one step hopping with a pre-scheduled hopping pattern. Finally, a state space equation is made by linearization of the Poincare map, and the control law for the foot placement is calculated by the pole placement method. The similar concept was used in the passive dynamic walker [6].

This paper is organized as follows: In Section 2, the simple model and dynamics are explained. In Sections 3, the foot placement strategy for stabilization is addressed. In Section 4, the overall strategy for stabilization and experiment are explained. Finally, the last section concludes the paper.

II. Model and Dynamics

A humanoid robot consisting of many numbers of links and actuators has been simplified. A generally used model is a linear inverted pendulum model. S. Kajita et al. used this model for the biped locomotion [2] and J. Pratt et al. used a more advanced model having a flywheel [5]. Similarly, T. Komura et al. used an angular momentum pendulum model [11]. Also, Hyon et al. [7] and C. Chevallereau et al. [12] used different types of a five-link model.

In this paper, the simple model consisting of four links is proposed in Figure 2. It is a similar to the telescopic compass-like biped walker model [22]. Each leg doesn't have the sole and is composed of two links and one actuator. And, a length of both legs, l_1 and l_2, can be changed. Also, a rotational actuator is located between both legs and is related to q_2. An angle with respect with the vertical line is defined as q_1. To consider the effect of mass distribution of real robot, it is assumed that the simple model is composed of mass of upper-body (M_h) and mass of each foot (m). For convenience, it is assumed that there is no inertia. Even though many studies use mass-less model in the foot, mass of the foot affects the dynamics of the robot largely in the real environment when the robot moves the swing leg to change the foot placement. Therefore, mass of the foot is introduced in this paper. Also, it is assumed that every actuator follows the desired trajectories perfectly. Since the real humanoid robot uses high ratio reducer gear, this assumption can be accepted.

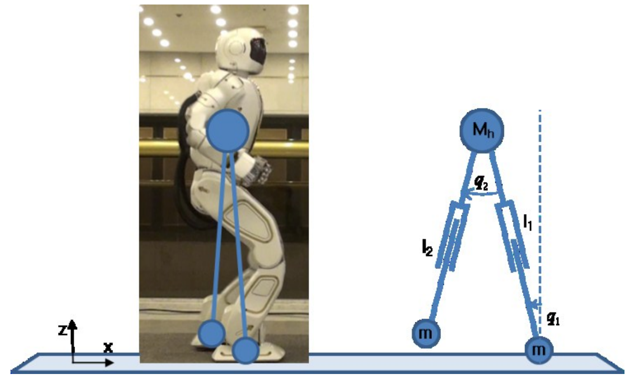

Figure 2. Simple model of a humanoid robot

Since this study deals with hopping of the humanoid robot, this model is a hybrid system composed of a stance phase model, a flight phase model, and an impact model. Dynamic equation of a stance phase model is as below.

$$M_s(q_s)\ddot{q}_s + C_s(q_s,\dot{q}_s) + G_s(q_s) = \tau_s \qquad (1)$$

where M_S is the 4 by 4 mass matrix, C_S is the vector containing Coriolis and centripetal terms, G_S is the vector containing gravitational terms, τ_S is the vector containing torque and force terms, and q_S is the state vector, $[q_1\ q_2\ l_1\ l_2]^T$.

On the other hand, dynamic equation of a flight phase model is as below.

$$M_f(q_f)\ddot{q}_f + C_f(q_f,\dot{q}_f) + G_f(q_f) = \tau_f \qquad (2)$$

where M_f is the 6 by 6 mass matrix for flight phase, q_f is the state vector, $[q_1\ q_2\ l_1\ l_2\ x_0\ z_0]^T$, the other are similar to them for stance phase.

Finally, an impact model is below.

$$\dot{q}_s^+ = \Delta(\dot{q}_f^-) \qquad (3)$$

where $\dot{q}_s^+$ is the derivate state vector for stance phase model just after impact and $\dot{q}_s^-$ is the derivate state vector for flight phase model just before impact.

With Equations (1) – (3), a Poincare map for one step hopping, F is made.

$$x_{k+1} = F(x_k, u_k), \qquad (4)$$

$$\text{where } x_k = [q_{s,k} \quad \dot{q}_{s,k}]^T.$$

Here, x is the initial condition of each hopping, k means k-th hopping, and u_k is an input.

III. Controller for Stable Hopping (Foot Replacement Strategy)

A. Linearization of Poincare Map

If a Poincare map outputs the same value from the specific input, that is, a fixed point, a humanoid robot can do periodic locomotion, such that

$$x^* = F(x^*, u^* = 0). \qquad (5)$$

To make a controller for stable hopping, equation 4 is linearized at the fixed point as below.

$$x_{k+1} = F(x_k, u_k)$$
$$\approx F(x^*, u^*) + \left.\frac{\partial F(x,u)}{\partial x}\right|_{x^*, u=0} (x_k - x^*) + \left.\frac{\partial F(x,u)}{\partial u}\right|_{x^*, u=0} u_k ,$$
where $e_k = x_k - x^*$,

Thus, upper equation can be expressed as the following state space equation.

$$e_{k+1} = Ae_k + Bu_k \tag{6}$$

where $A = \left.\frac{\partial F(x,u)}{\partial x}\right|_{x^*, u=0}$ and $B = \left.\frac{\partial F(x,u)}{\partial u}\right|_{x^*, u=0}$

B. *Design of Controller*

For hopping motion of the robot, the hopping pattern designed in the previous study is applied [13]. Since it is assumed that all actuators follow the desired trajectories perfectly, equation 6 is reduced to the following equation.

$$e_{k+1}^{reduce} = A^{reduce} e_k^{reduce} + B^{reduce} u_k^{reduce} \tag{7}$$

where $e_k^{reduce} = [q_1 \quad \dot{q}_1]^T$

And, u_k^{reduce} means the final angle between both legs. Therefore, equation 7 becomes a general state space equation. A controller law is calculated by the pole placement method. For the pole placement method, following MATLAB function is used.

$$k = place(A^{reduce}, B^{reduce}, P)$$

where $P = [p_1 \quad p_2]^T$

p_1 and p_2 are desired pole of the controlled system, and are set to smaller than one. Finally, controller law is as followed.

$$u_k = -k * e_k^{reduce} \tag{8}$$

Proposed controller is verified by the simulation.

A humanoid robot used in this paper is HUBO2 developed at KAIST. For the similarity between the real robot model and the simplified model, the parameters of the simplified model are set in Table 1. Considering the mass distribution, mass of the upper body (M_h) is set to 34 kg and mass of each foot (m) is set to 3 kg. Also, since the length from a hip joint to a foot is 0.48 m when the robot takes the hopping ready position, the initial length of each leg is 0.48m.

Table 1. Parameters for the simplified model

Upper-body(M_h)	34kg
foot(m)	3kg
Total mass	40kg
Length of leg(l_1 & l_2)	0.48m

As an example, P vector can be set as below.

$$P = [0.4 + j0.4 \quad 0.4 - j0.4]^T$$

To verify the stability of the proposed method, many simulations are carried out according to the different initial conditions. Figure 3 – 5 show the simulation results. Figure 3 is the phase portrait when the initial condition has the only position difference from the fixed point value, [10 degree, 0 radian/second]. The graph converges to the origin as the step progresses. In Figure 6, the circled graph means the final angle between both legs in this situation. By the initial error, the final angle became 16 degree, but it is gradually decreased to zero. Figure 4 shows the phase portrait when there is only velocity error in the initial condition. Like Figure 3, the graph converges to zero as time passes. Also, Figure 5 shows the phase portrait when there are position and velocity differences together in the initial condition. It also converges to zero well. In Figure 6, the stared graph and the rectangle graph show the final angle between both legs according to the initial conditions of Figure 4 and 5. That is, the robot converges to fixed point with respect to various initial errors.

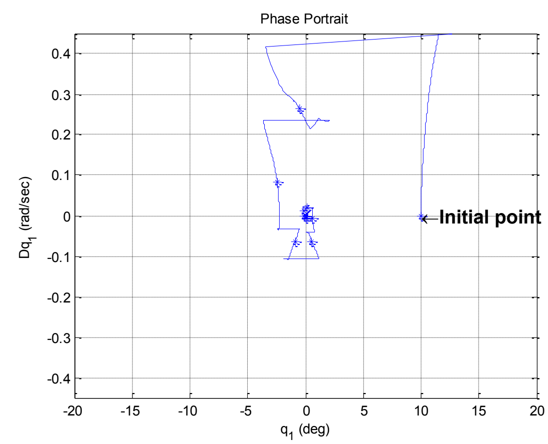

Figure 3. Simulation Result for initial condition

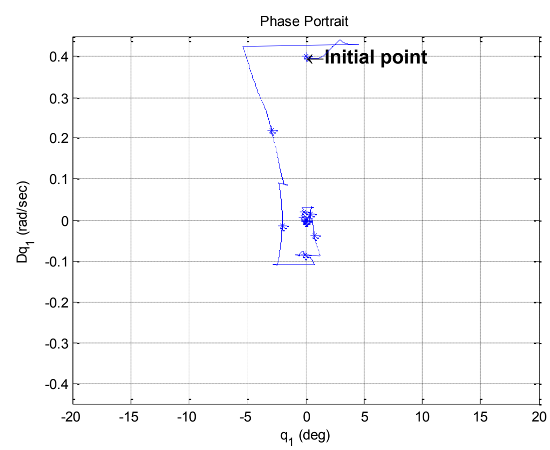

Figure 4. Simulation Result for initial condition

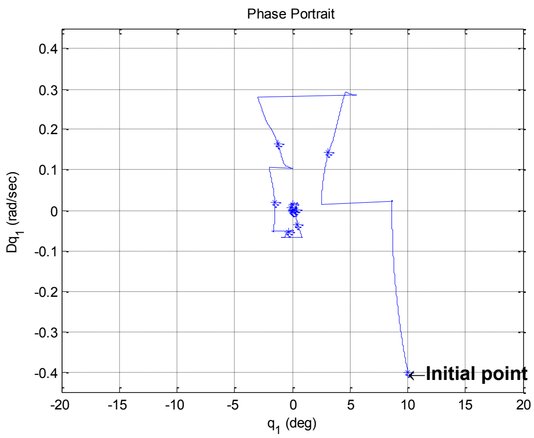

Figure 5 . Simulation Result for initial condition

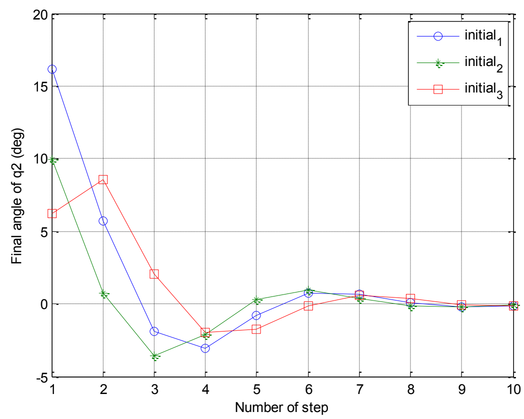

Figure 6. Variation of the input, final angle of q_2 according to initial conditions.

IV. OVERALL STRATEGY FOR STABILIZATION AND EXPERIMENT

Theoretically, the proposed method in the previous section is enough to make stabilization against disturbance such as push. However, since the real environment is different from the simulation environment, the real experiment result is also different from the simulation. For example, a signal of the inertia measurement unit (IMU) has a drift, and is influenced by a vibration and an impact of the robot. Therefore, two controllers are proposed to make stable push recovery in the real experiment. If disturbance is small, the robot maintains stability through the posture balance controller mentioned the previous study [10]. On the other hand, if disturbance is large, the posture balance controller and the foot placement method are used together.

The size of disturbance is distinguished by the ZMP. If the ZMP is placed within the sole of a humanoid robot, disturbance is small. Otherwise, disturbance is large. The ZMP can be estimated by the IMU.

$$ZMP = \frac{l^2\ddot{q}_1 + gl\sin q_1}{-l\cos q_1\dot{q}_1^2 - l\sin q_1\ddot{q}_1 + g} \tag{9}$$

Because the distances from the ankle joint to the toe and heel are 140 mm and 80mm, if the estimated ZMP is located between -80 mm and 140 mm, the posture balance control is activated. If the estimated ZMP is escaped that range, the foot placement method is activated like Figure 7. Thus, the switch for the foot placement control is set to

$$\text{Switch} = \begin{cases} \text{OFF}, -80\text{mm} \le ZMP \le 140\text{mm} \\ \text{ON, else} \end{cases} \tag{10}$$

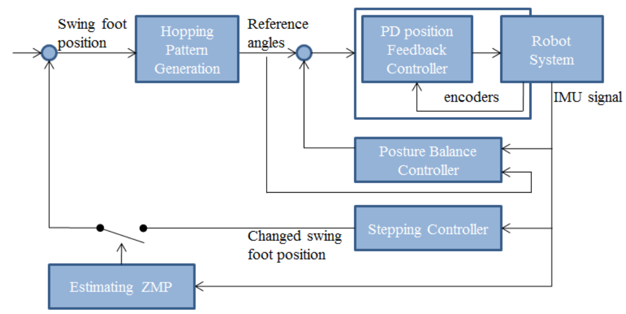

Figure 7. Overall strategy for stabilization

A. *Summary of posture balance control for small disturbance*

As mentioned before, the posture balance controller is used for small disturbance. The control law of posture balance control is as given below.

$$\begin{aligned} u_{AnklePitch} &= \theta^{Ref}_{AnklePitch} + \theta^{Control}_{AnklePitch} \\ &= \theta^{Ref}_{AnklePitch} + C_{Filter}K_P(\theta^{Ref}_{AnklePitch} - \theta^{IMU}_{AnklePitch}) \end{aligned} \tag{11}$$

$\theta^{Ref}_{AnklePitch}$ means the pre-scheduled ankle trajectory in the hopping pattern generation, $\theta^{Control}_{AnklePitch}$ means the control input created by the posture balance controller. The posture balance controller uses a P-controller. The structure of the posture balance controller in the sagittal plane is shown in Figure 6.

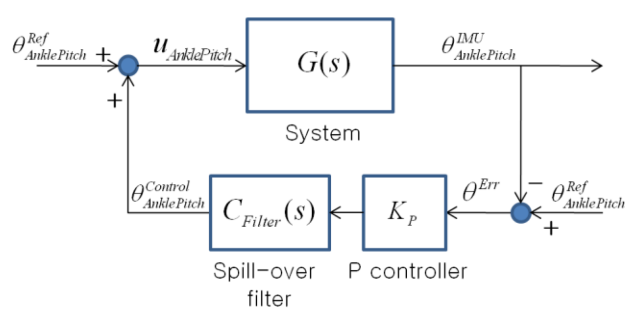

Figure 8. Block diagram of the posture balance control

The proposed controllers were applied to the humanoid robot, HUBO2 when small disturbance is applied. Figure 9 is snap shots of the balancing experiment for small disturbance when the HUBO2 hops in place. As shown in the sixth picture of Figure 11, HUBO2 was pushed slightly. However, the robot maintained the stability through the posture balance control, not the landing position control. It is worthy of attention that the robot doesn't change the foot placement of the swing foot. It will be explained in next section.

B. Experiment of foot placement control for large disturbance

If disturbance is large, the proposed foot placement controller is used. As mentioned the previous section, the foot placement control is activated according to the estimated ZMP. Even though the range for the foot placement control is Equation 12, we decreased the range to obtain the margin. Thus, the range is reduced to 30%, which is decided by the trial and error. That is, the range for the foot placement control is

$$\text{Switch} = \begin{cases} \text{OFF}, -0.024\text{m} \le \text{ZMP} \le 0.042\text{m} \\ \text{ON, else} \end{cases}. \quad (12)$$

Figure 9 shows the estimated ZMP when the HUBO2 hops with controllers. Since the HUBO2 was pushed about 4.62 seconds, the ZMP was changed largely. And, the ZMP was escaped the range in Equation 12. Thus, the foot placement control was activated. Figure 10 shows the trajectories of hip pitch joints when the robot hops. The trajectories were changed from 4.62 seconds to 5.28 seconds because of the foot placement control. Finally, Figure 12 shows the snap shots of the experiment of the foot placement control. The HUBO2 pushed in the 4^{th} picture, and the landing position of the swing foot was changed from the 5^{th} to the 8^{th} pictures. With the foot placement control, the HUBO hop in place well against the large disturbance.

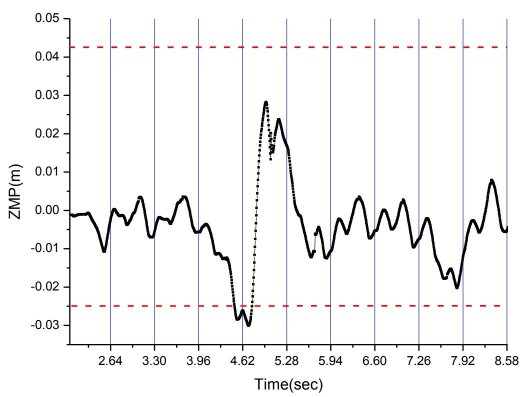

Figure 9. Estimated ZMP of the robot. The estimated ZMP, which is estimated by the IMU signal, is escaped the lower criteria for the landing position controller. Therefore, the landing position controller is activated.

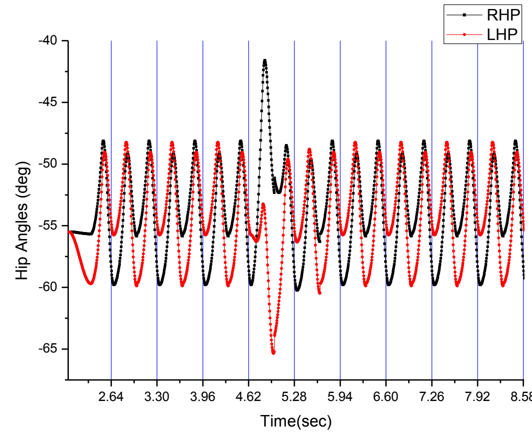

Figure 10. Desired trajectories of both hip pitch joints. LHP denotes a joint of the left hip pitch and RHP is right one. Because the landing position controller is activated, the trajectory for hopping is changed for the next step after activating the controller.

V. CONCLUSIONS

In this paper, the stabilization of the hopping humanoid robot against disturbance was addressed. For the stabilization of the robot, the novel foot placement strategy was proposed, and verified through the experiment. The foot placement control is the method to change the landing position of the swing foot with the Poincare-map of the simplified model. Even though, theoretically the robot can make a balance with only the foot placement method, the real humanoid robot used the posture balance control and the foot placement strategy for the stabilization because of the real environmental reasons.

In future work, more precise controller will be proposed with more complicated model similar to the real robot. Also, this proposed concept will be applied to running humanoid robot to make stable running against disturbance.

REFERENCES

[1] A. Hofmann, Robust execution of bipedal walking tasks from biomechanical principles, Ph.D. dissertation, Massachusetts Institute of Technology, January 2006.

[2] S. Kajita and K. Tani, Study of dynamic biped locomotion on rugged terrain – derivation and application of the linear inverted pendulum mode, in *IEEE 1991 International Conference on Robotics and Automation (ICRA)*, pp. 1405-1411.

[3] Ill-Woo Park, Jung-Yup Kim, Jung-Ho Lee, and Jun-Ho Oh, Mechanical Design of Humanoid Robot Platform KHR-3 (KAIST Humanoid Robot-3: HUBO), in *5th IEEE-RAS International Conference on Humanoid Robots*, pp. 321-326, 2005.

[4] S. Kajita, T. Nagasaki, K. Kaneko, K. Yokoi and K. Tanie, A Running Controller of Humanoid Biped HRP-2LR, in *IEEE ICRA* (2005), pp. 618-624.

[5] Jerry Pratt, John Carff, Sergey Drakunov, and Ambarish Goswami, Capture Point: A Step toward Humanoid Push Recovery, in *IEEE-RAS International Conference on Humanoid Robots*, 2006.

[6] Arthur D. Kuo, Stabilization of Lateral Motion in Passive Dynamic Walking, *International Journal of Robotics Research* 18(9) (1999), pp. 917-930.

[7] Sang-Ho Hyon and Takashi Emura, Symmetric Walking Control: Invariance and Global Stability, *in Proc. of IEEE International Conference on Robotics and Automation (2005),* pp. 1455-1462.

[8] Marc H. Raibert, *Legged Robots That Balance* (MIT Press, Cambridge, Massachusetts, 1986).

[9] Sang-Ho Hyon, Joshua G. Hale, and Gordon Cheng, Full-Body Compliant Human-Humanoid Interaction: Balancing in the Presence of Unknown External Forces, *IEEE Transactions on Robotics*, vol. 23, no. 5, Oct., 2007.

[10] Baek-Kyu Cho, Sang-Sin Park, and Jun-Ho Oh, Controllers for Running in the Humanoid Robot, HUBO, *in Proc. of IEEE/RAS International Conference on Humanoid Robots*, 2009.

[11] T. Komura, A. Nagano, H. Leung, and Y. Shinagawa, Simulating pathological gait using the enhanced linear inverted pendulum model, *IEEE Transactions on Biomedical Engineering 52(9) (2005)*, pp 1502-1513.

[12] C. Chevallereau, E.R. Westervelt and J.W. Grizzle, Asymptotically Stable Running for a Five-link, Four-actuator, Planar Bipedal Robot, *Intr. J. of Robotics Research* 24(6) (2005), pp. 431-464.

[13] Baek-Kyu Cho, Ill-Woo Park, and Jun-Ho Oh, Running Pattern Generation of Humanoid Biped with a Fixed Point and Its Realization, *International Journal of Humanoid Robotics*, volume 6, Issue 4, pp. 631-656, 2009.

[14] "The Honda Humanoid Robot ASIMO." Available: http://world.honda.com/ASIMO/

[15] Ryoske Tajima, Daisaku Honda, and Keisuke Suga, Fast Running Experiments Involving a Humanoid Robot, in *2009 IEEE International Conference on Robotics and Automation (ICRA)*, pp. 1571-1576, 2009.

[16] T. Ishida, Development of a Small Biped Entertainment Robot QRIO, in *Int. Symp. On Micro-Nanomechatronics and Human Science*, pp. 23-28, 2004.

[17] Benjamin Stephens, Humanoid Push Recovery, in *IEEE-RAS International Conference on Humanoid Robots*, 2007.

[18] R. Tajima and K. Suga, Motion Having a Flight Phase: Experiments Involving a One-legged Robot, in *Int. Conf. on Intelligent Robots and Systems* (2006), pp.1726-1731.

[19] S. Kajita, T. Nagasaki, K. Kaneko, K. Yokoi and K. Tanie, A Running Controller of Humanoid Biped HRP-2LR, in *IEEE ICRA* (2005), pp. 618-624.

[20] M. Vukobratovic and B. Borovac, Zero-moment point – thirty five years of its life, *International Journal of Humanoid Robotics*, vol. 1, 2004, pp. 157-173.

[21] S. Kajita, F. Kanehiro, K. Kaneko, K. Fujiwara, K. Harada, K. Yokoi and H. Hirukawa, Resolved Momentum Control: Humanoid Motion Planning Based on the Linear and Angular Momentum, in *IEEE IROS (2003)*, pp. 1644-1650.

[22] S. Miyakshi and G. Cheng, Examining Human Walking Characteristics with a Telescopic Compass-like Biped Walker Model, in IEEE International Conference on Systems, Man and Cybernetics, pp. 1538-1543, 2004.

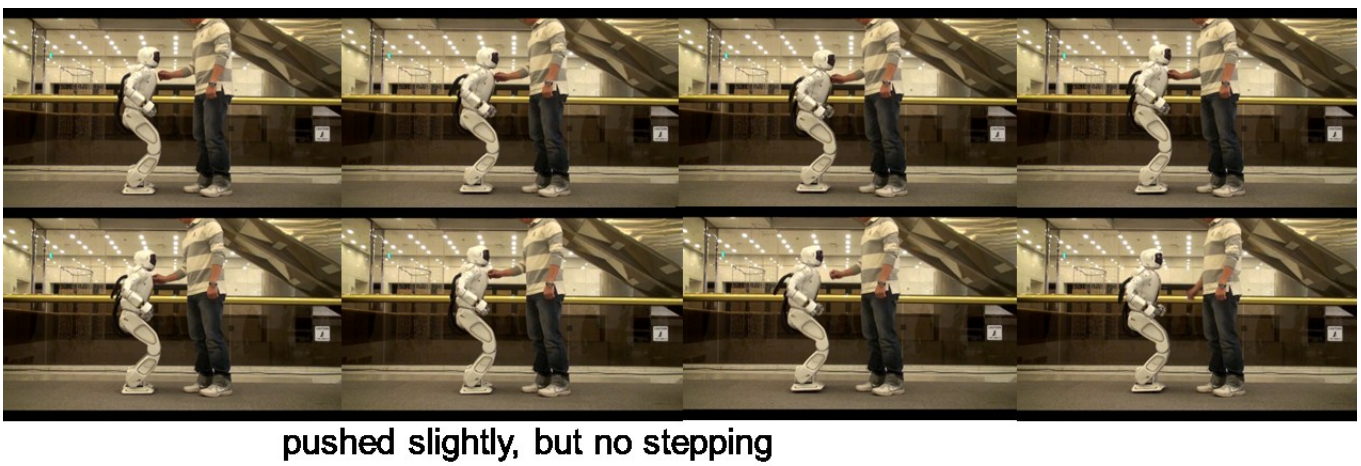

Figure 11. Snap shots of the balancing experiment for small disturbance

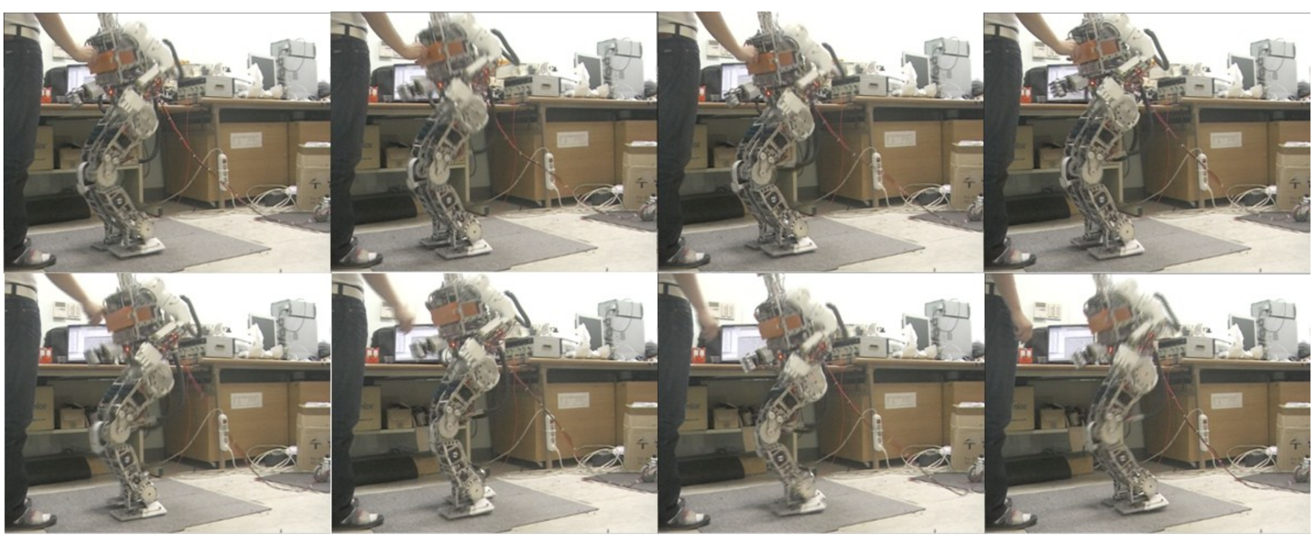

Figure 12. Snap shots of the foot placement control. After pushing (4th picture), HUBO2 exchanges the landing position of the swing foot (6th picture).